Design and Implementation of an Extended Kalman Filter for Sensorless Control of a Permanent Magnet Synchronous Motor without Phase Voltage Measurement

G. Terörde, K. Hameyer, G. Deconinck* and R. Belmans
Katholieke Universiteit Leuven; Dep. E.E./ESAT-ELEN, (*ESAT-ACCA)
Kardinaal Mercierlaan 94, B-3001 Leuven, Belgium
E-mail: gerd.teroerde@esat.kuleuven.ac.be

Abstract – The system studied in this paper is a sensorless control of a permanent magnet synchronous motor (PMSM). Its structure is based on the extended Kalman filter theory using only the measurement of the motor current for the on-line estimation of speed and rotor position. The speed-controlled PMSM is supplied by a voltage source PWM inverter. The PWM generation is done by space vector modulation. The motor voltages necessary for the Kalman algorithm are calculated with consideration of the non-linearity of the inverter. Sophisticated control rules such as Kalman filtering in real time require a very fast signal processor specially adapted to perform complex mathematical calculations. As digital signal processors have become cheaper and their performance greater, it has become possible to use them as a cost-effective solution. The filter design and the real-time implementation issues of a sensorless control using a TMS320C31 DSP for the main control are presented. The I/O subsystem and the PWM generation are based on a TMS320P14 working as a slave-DSP. Finally, an evaluation of the experimental results is presented.
Keywords: machine control, Kalman Filter

1. System Model

The system considered is a permanent magnet synchronous motor (PMSM) having permanent magnets mounted on the rotor. The resulting back-EMF voltage induced in each stator phase winding during rotation can be modelled quite accurately as a sinusoidal waveform. A block diagram of the speed and position estimator is shown in figure 1.

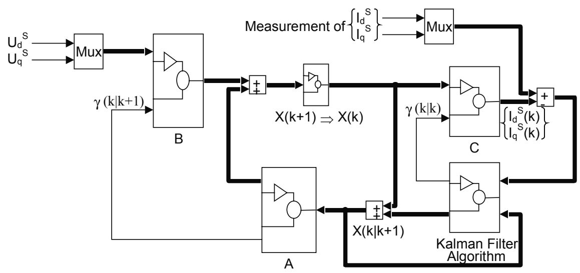

Figure 1: Block diagram of the discrete motor model and extended Kalman filter.

The Kalman filter is based on a machine model in (discrete-time) state space. The dynamic model for the PMSM in a stator-fixed reference frame (indices: 's'), choosing the rotor-fixed current i_d, i_q, the angular velocity ω_e, and the rotor position γ as state variable $\underline{x}_k$ and the fundamental voltage as input $\underline{u}_k$, is described by equations (1)-(5). This model assumes the velocity ω_e to be constant in a small time interval (sampling time T_s). The motor parameters are:

- R_1 stator per-phase resistance
- $L_{d,q}$ d,q axis inductance
- ψ permanent magnet flux linkage

$$\underline{x}_{k+1} = \underline{A}(\underline{x}_k)\cdot\underline{x}_k + \underline{B}(\underline{x}_k)\cdot\underline{u}_k\ ;\quad \underline{x}_k = \begin{pmatrix} i_d \\ i_q \\ \omega_e \\ \gamma \end{pmatrix}_k ;\quad \underline{u}_k = \begin{pmatrix} U_d^s \\ U_q^s \end{pmatrix}_k \tag{1}$$

with:

$$\underline{A}(\underline{x}_k) = \begin{pmatrix} 1 - R_1\dfrac{T_s}{L_d} & \omega_e T_s\dfrac{L_q}{L_d} & 0 & 0 \\ -\omega_e T_s\dfrac{L_d}{L_q} & 1 - R_1\dfrac{T_s}{L_q} & -T_s\dfrac{\Psi}{L_q} & 0 \\ 0 & 0 & 1 & 0 \\ 0 & 0 & T_s & 1 \end{pmatrix} \tag{2}$$

$$\underline{B}(\underline{x}_k) = \begin{pmatrix} T_s\dfrac{\cos(\gamma)}{L_d} & T_s\dfrac{\sin(\gamma)}{L_d} \\ -T_s\dfrac{\sin(\gamma)}{L_q} & T_s\dfrac{\cos(\gamma)}{L_q} \\ 0 & 0 \\ 0 & 0 \end{pmatrix} \tag{3}$$

The resulting output vector $\underline{y}_k$ consists of the estimated motor current in a stator-fixed reference frame:

$$\begin{pmatrix} I_d^s(k) \\ I_q^s(k) \end{pmatrix} = \underline{y}_k = \underline{C}(\underline{x}_k)\cdot\underline{x}_k \tag{4}$$

$$\underline{C}(\underline{x}_k) = \begin{pmatrix} \cos(\gamma) & -\sin(\gamma) & 0 & 0 \\ \sin(\gamma) & \cos(\gamma) & 0 & 0 \end{pmatrix} \tag{5}$$

The output vector is compared to the measured current vector. The difference is used to correct the state vector of the system model.

The state space model is non-linear due to the cross product of the state variable $\underline{x}_k$. Consequently a nonlinear filter, such as the extended Kalman Filter (EKF), will be implemented. In fact, it is impossible to prove the convergence of the model [1].

2. PHASE VOLTAGE

The extended Kalman filter algorithm requires the motor voltages as input. An alternative to the complex measurement and filtering of the motor voltage is the use of the reference voltage for the PWM, available at the output of the current control. The PWM generation is performed by space vector modulation (SVM). The SVM minimizes the harmonic content determining the copper losses of the machine, accounting for a major portion of the machine losses. SVM also provides a more efficient use of the supply voltage in comparison to sinusoidal modulation methods. The homopolar system containing in the phase voltages, shown at different modulation indices in Fig. 2, must be considered in the Park transformation.

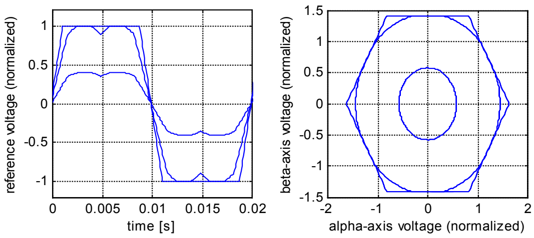

Figure 2: shape of the reference voltage at modulation index m = 0.5, m = 1.25 and m =2 (frequency = 50Hz).

In case of an ideal inverter, which is composed of lossless and delay-free switching elements, the filtered phase voltage U assumes the shape of the reference voltage. With the reference x_{ref} it implies that U corresponds to:

$$U = \frac{U_c}{2} \cdot x_{ref} \text{ , } \quad U_c = \text{DC bus voltage , } |x_{ref}| \leq 1 \tag{6}$$

It was assumed that the inverter switches behave ideally. This is not true for almost all semiconductor switches reacting delayed to their control signals at turn-on and turn-off. The phase voltages are strongly deviating from the reference voltages. This leads in the Kalman filter algorithm to large position and speed errors. At low motor speed the control becomes even unstable. With positive current the duty cycles are shorter, with negative current they are longer than required. Hence, the actual duty cycle of a bridge is always different from that of the reference voltage. It is either increased or decreased, depending on the load current polarity. This effect is described by an error voltage ΔU

$$\Delta U \approx \frac{U_T + U_D}{2} + t_d \cdot f_{PWM} \cdot U_c \tag{7}$$

dependent on the dead-time t_d, the dc-bus voltage U_c, the PWM-frequency f_{PWM} and the voltages U_D and U_T at transistor and diode [2]. This and the resistant R_T and R_D of the switch changes the inverter output from its intended value U_{ref} to

$$U \approx U_{ref} - I \cdot \frac{R_{T1} + R_D}{2} - \Delta U \cdot \text{sign}(I) \text{ ,} \tag{8}$$

used as input of the Kalman filter algorithm.

3. EXTENDED KALMAN FILTER ALGORITHM

The state model of the PMSM is non-linear. The electrical speed and the position of the rotor are considered as both, state and parameter. The model matrices $\underline{B}$ and $\underline{C}$ depend on the position of the rotor, the matrix $\underline{A}$ on the electrical speed. Therefore, the extended Kalman filter (EKF) has to be used to estimate the parameters of the model matrices, as well. The EKF re-linearises the non-linear state model for each new estimation step, as it becomes available. Furthermore, the EKF provides a solution that directly cares for the effects of measurement or system noise. The errors in the parameters of the system model will also handled as system noise.

The optimal state estimation $\underline{x}_{k|k}$ generated by the EKF is achieved, as

$$\sum_{i=1}^{n} E\left\{\tilde{x}_i^2\right\} \text{, E\{\} = expected values} \tag{9}$$

is minimized [1]. In [3] a recursive algorithm is presented for the discrete time case to provide the solution for this equation. The signal flow of the EKF in a recursive manner is shown in figure 3.

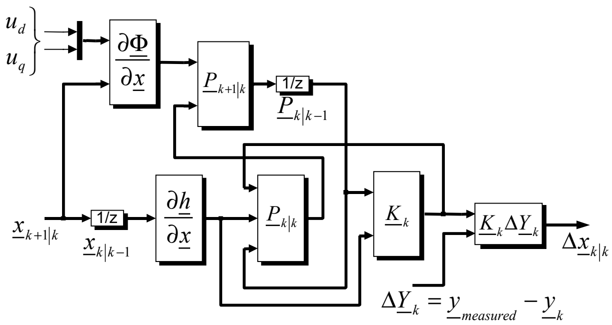

Figure 3: Block diagram of the extended Kalman filter (EKF).

It has to be distinguished between the filter and predictor equations. The predicted value of the state vector $\underline{x}_{k+1|k}$ is corrected by multiplying the filter gain and the difference between estimated and measured output vector $\underline{y}_k$ to the state vector $\underline{x}_{k|k}$. In addition still the equation for the corrected covarianz matrix $\underline{P}_{k|k}$ is required.

$$\underline{x}_{k|k} = \underline{x}_{k|k-1} + \underline{K}_k \left(\underline{y}_k - \underline{h}\left(\underline{x}_{k|k-1}, k \right) \right) \tag{10}$$

$$\underline{P}_{k|k} = \underline{P}_{k|k-1} - \underline{K}_k \frac{\partial h}{\partial \underline{x}} \Big|_{\underline{x} = \underline{x}_{k|k-1}} \underline{P}_{k|k-1} \tag{11}$$

The matrix $\underline{K}_k$ is the feedback matrix of the extended Kalman filter (EKF). This matrix determines how the state vector $\underline{x}_{k|k}$ is modified after the output of the model $\underline{y}_k$ is compared to the measured output of the system. The filter gain matrix is defined by:

$$\underline{K}_k = \underline{P}_{k|k-1} \frac{\partial h^T}{\partial \underline{x}} \Big|_{\underline{x} = \underline{x}_{k|k-1}} \left(\frac{\partial h}{\partial \underline{x}} \Big|_{\underline{x} = \underline{x}_{k|k-1}} \underline{P}_{k|k-1} \frac{\partial h^T}{\partial \underline{x}} \Big|_{\underline{x} = \underline{x}_{k|k-1}} + \underline{R} \right)^{-1} \tag{12}$$

in which $\underline{R}$ is based on the covariance matrix of the measurement noise.

Based on the calculated state vector $\underline{x}_{k|k}$, a new value of the state vector can be predicted. The same applies to the error covariance matrix. The prediction is given by

$$\underline{x}_{k+1|k} = \underline{\Phi}\left(k+1,k,\underline{x}_{k|k-1},\underline{u}_k\right) \tag{13}$$

$$\underline{P}_{k+1|k} = \frac{\partial \underline{\Phi}}{\partial \underline{x}}\Big|_{\underline{x}=\underline{x}_{k|k}} \underline{P}_{k|k} \frac{\partial \underline{\Phi}^T}{\partial \underline{x}}\Big|_{\underline{x}=\underline{x}_{k|k}} + \underline{\Gamma}_k \underline{Q} \underline{\Gamma}_k^T \tag{14}$$

with the covariance matrix $\underline{Q}$ of the system noises. The system vector $\underline{\Phi}$ and the output vector $\underline{h}$ respectively can be derived from the model equations of the PMSM.

$$\underline{\Phi}\left(k+1,k,\underline{x}_{k|k-1},\underline{u}_k\right) = \underline{A}_k\left(\underline{x}_{k|k}\right)\underline{x}_{k|k} + \underline{B}_k\left(\underline{x}_{k|k}\right)\underline{u}_{k|k} \tag{15}$$

$$\underline{h}\left(\underline{x}_{k|k-1},k\right) = \underline{C}_k\left(\underline{x}_{k|k-1}\right)\underline{x}_{k|k-1} \tag{16}$$

$$\frac{\partial \underline{h}}{\partial \underline{x}} = \begin{pmatrix} \cos(\gamma) & -\sin(\gamma) & 0 & -i_d\sin(\gamma) - i_q\cos(\gamma) \\ \sin(\gamma) & \cos(\gamma) & 0 & i_d\cos(\gamma) - i_q\sin(\gamma) \end{pmatrix} \tag{17}$$

$$\frac{\partial \underline{\Phi}}{\partial \underline{x}} = \begin{pmatrix} 1 - R_1\frac{T_s}{L_d} & \omega_e T_s \frac{L_q}{L_d} & T_s\frac{L_q}{L_d} i_q & \frac{T_s}{L_d} u_q \\ -\omega_e T_s \frac{L_d}{L_q} & 1 - R_1\frac{T_s}{L_q} & -\frac{T_s}{L_q}\left(L_d i_d + \Psi\right) & -\frac{T_s}{L_q} u_d \\ 0 & 0 & 1 & 0 \\ 0 & 0 & T_s & 1 \end{pmatrix} \tag{18}$$

where u_q and u_d are voltages in a rotor-fixed reference frame.

4. Covariance Matrices

The critical step in the EKF is the search for the best covariance matrices. $\underline{Q}$ and $\underline{R}$ have to be set-up based on the stochastic properties of the corresponding noise. The noise covariance $\underline{R}$ accounts for the measurement noise introduced by the current sensors and the quantization errors of the A/D converters. Increasing $\underline{R}$ indicates stronger disturbance of the current. The noise is weighted less by the filter, causing also a slower transient performance of the system.

The noise covariance $\underline{Q}$ reflects the system model inaccuracy, the errors of the parameters and the noise introduced by the voltage estimation. $\underline{Q}$ has to be increased at stronger noises driving the system, entailing a more heavily weighting of the measured current and a faster transient performance.

The initial covariance matrix $\underline{P}_0$ represents mean squared errors in knowledge of the initial conditions. Varying $\underline{P}_0$ affects neither the transient performance nor the steady state conditions of the system.

In general, the entries of the covariance matrices $\underline{Q}$ and $\underline{R}$ are unknown and can not be calculated. They are often set equal to the unity matrix. In order to achieve a good filter performance, they must be filled based on experimental investigations. This covers an iterative process for searching the best values.

In the following experiments, the best filter performance was obtained with

$$\underline{R} = \underline{\mathbf{I}};\ Q_{11} = Q_{22} = Q_{33} = 0.03;\ Q_{44} = 7\cdot 10^{-5};\ \underline{P}_0 = 0.02\cdot\underline{\mathbf{I}}$$

whereby $\underline{\mathbf{I}}$ is the identity matrix. $\underline{Q}$, $\underline{R}$ and $\underline{P}_0$ are assumed to be diagonal.

5. Experimental Results

The turnaround time of the entire control system amounts to 227 µs and the used sample time is T_s =250 µs. Figure 4 shows the experimental result of a speed reversal using the estimated speed and position as feedback. Additionally, the real speed and position are measured and compared.

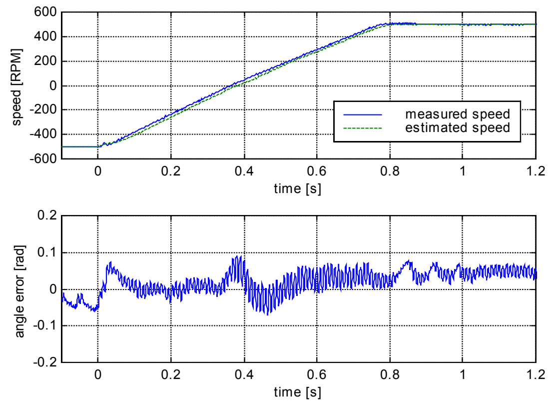

Figure 4: Speed reversal test. Above: Measured and estimated speed. Below: Error of the angle estimation.

It can be seen that there is a very good coincidence between real and estimated speed and position respectively. Figure 5 presents the response of the PMSM to a load step at a motor speed of 1000 RPM. The applied load amounts to 70% of the rated torque. The current controller, using also the estimated values of d- and q-axis current, has a bandwidth of 926 Hz.

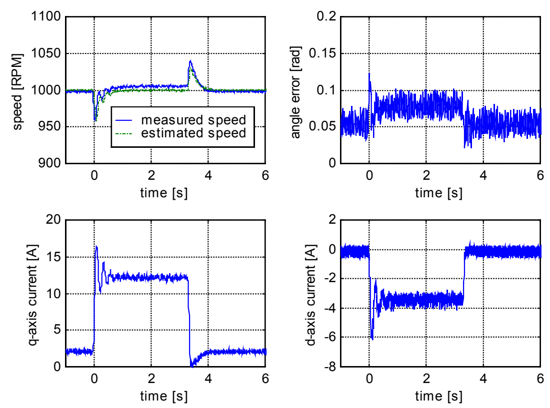

Figure 5: Load step at time 0 and 3.2 s (70% of the rated torque). Above: Speed and angle error. Below: Estimated q- and d-axis current.

The load disturbance creates a small speed error about 0.5%. This error is caused by the voltage estimation, depending on the dead-time and resistance of the switches. The steady state error can be further reduced by generating an offset for the speed reference using the frequency of the measured current. The angle error is negligibly.

At low motor speed ($\omega \Rightarrow 0$) the equations of the PMSM are simplified as the voltage induced by the magnets is very small. Thus, no more predicate can be made over the position of the magnets and the EKF fails. Since at standstill only dc-values are given, the necessary flux variation must be forced by impressing a test signal into the system. A signal, which can be implemented easily, represents an additionally sinusoidal reference current in the d-axis of the motor, using the d/q axis-symmetrie of the rotor to estimate the real position. In all presented experimental results the following d-axis reference current is used:

$$i_{d,ref} = i_d^* + 5\mathrm{A}\,\sin(2\pi\, 200\frac{1}{\mathrm{s}}\, t)\cdot\left(1-\frac{|n|}{500\mathrm{RPM}}\right),\ n = \text{speed} \quad (19)$$

whereby i_d^* results from the speed control. Figure 6 presents the response of the d- and q-axis current to a step of the speed reference from standstill to 1000 RPM. The corresponding speed is shown in figure 7, marked as “EKF, negative d-axis current”.

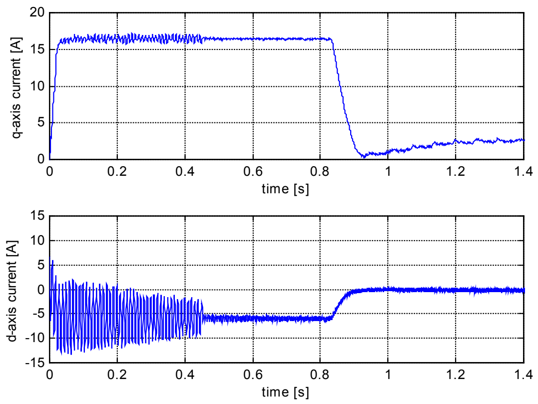

Figure 6: Current at a speed step (see Fig. 7)
Above: q-axis current. Below: d-axis current.

The generated reluctance torque is compensated by a complementary q-axis current. Nevertheless, further investigations about the optimal frequency and magnitude of the additionally d-axis current has to be made.

The electromagnetic torque T_e can be expressed as:

$$T_e = p\left[\Psi\, i_q - \left(L_q - L_d\right) i_d\, i_q\right] \quad (20)$$

The optimal control of the motor takes advantage of the reluctance torque by introducing a negative ($L_d < L_q$) direct axis current component. In figure 7 a comparison is given of motor control with feedback of the estimated speed and optimum d-axis current, motor control with feedback of the estimated speed and no d-axis current and motor control with feedback of the measured speed and position (FOC).

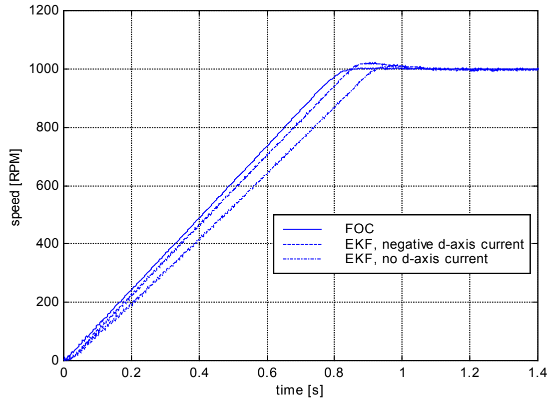

Figure 7: Speed step with feedback of the estimated speed and position (EKF), optimum d-axis current, no d-axis current and with feedback of the measured speed and position (FOC).

The reported filter algorithm was tested on a PMSM with the main drive parameters:

- I_n : rated current = 10.6 A
- p : number of pole pairs = 3
- Ψ : permanent magnet flux = 0.256 Vs
- L_d : d-axis inductance = 8.8 mH
- L_q : q-axis inductance = 15 mH
- J_r : inertia of the drive = 0.113 kgm^2

6. CONCLUSION

This paper has presented the design and the implementation for a speed-sensorless control of a PMSM using the extended Kalman filter. Measurement and filtering of the motor voltages are not required. Instead, the reference voltages for the PWM are used. Results of the dynamic and steady state behaviour of the extended Kalman filter are reported. The position of the drive can be estimated also at standstill permitting a position control of the PMSM. The difference to the motor control with speed measurement is very small.

ACKNOWLEDGEMENT

This research is supported by the Ministry of Economy of Flemish Region (IWT-Vliet). The authors are also grateful to the Belgian “Fonds voor Wetenschappelijk Onderzoek Vlaanderen” for its financial support of this work and the Belgian Ministry of Scientific Research for granting the IUAP No. P4/20 on Coupled Problems in Electromagnetic Systems.

REFERENCES

[1] C. Manes, F. Parasiliti, M. Tursini: “Comparative Study of Rotor Flux Estimation in Induction Motors with a Nonlinear Observer and the Extended Kalman Filter”, IECON 1994

[2] Bose, B. K.: "Power Electronics and Variable Frequency Drives", IEEE Press, New York, 1997.

[3] Brammer, Siffling: “Kalman-Bucy Filter, Deterministische Beobachtung und stochastische Filterung” R. Oldenbourg Verlag Muenchen, Wien 1994.

[4] Strejc, V.: "State space theory of discrete linear control", John Wiley & Sons, 1980.

[5] Rajashekara, K. S., Kawamura, A.: "Sensorless Control of Permanent Magnet AC Motors", IEEE IECON Proceedings, pp. 1589-1594, 1994.